J. Physiol. (1984), **356**, *pp.* 565–585
With 1 plate and 7 text-figures
Printed in Great Britain

MEMBRANE PATCHES AND WHOLE-CELL MEMBRANES: A COMPARISON OF ELECTRICAL PROPERTIES IN RAT CLONAL PITUITARY (GH_3) CELLS

BY J. M. FERNANDEZ*, A. P. FOX† AND S. KRASNE

From the Department of Physiology, Ahmanson Laboratory of Neurobiology, Jerry Lewis Neuromuscular Research Center, University of California, Los Angeles, CA 90024, U.S.A.

(*Received 27 January 1984*)

SUMMARY

1. A comparison has been made between the electrical properties of excised 'outside-out' patches and whole-cell membranes of GH_3 cells using the patch-pipette technique.

2. Despite a complicated surface morphology, which includes numerous microvilli, ruffles and blebs, high-resistance seals (typically $> 10^{11}$ Ω) were consistently formed between patch pipettes and GH_3 cell membranes.

3. When the internal solution contained 120 mM-CsF, outward currents through K channels were blocked and large Na channel currents were consistently observed in the whole-cell recording mode. Using the same solutions, single Na channel currents were readily observed in outside-out patches. Averaging patch currents yielded macroscopic currents showing the same voltage-dependent kinetics as those observed for the whole-cell membrane.

4. The current *vs.* voltage and inactivation time constant *vs.* voltage relationships for the Na channel shifted towards more negative potentials (25 mV or more) within approximately 30 min after going into the whole-cell recording mode. These same relationships could be measured for outside-out patches and their positions along the voltage axis coincided with the asymptotic values measured in the whole-cell mode.

5. When the internal solution contained 120 mM-*N*-methylglucamine fluoride and the external solution contained 150 mM-Tris chloride, no ionic channel currents could be observed either for whole-cell or outside-out patch membranes. Under these conditions, displacement currents induced by tetraphenyl borate (TPB) were recorded in both types of membranes. The total charge moved showed a sigmoidal dependence upon the applied voltage for both whole-cell and outside-out patch membranes. The charge *vs.* voltage relationship showed a shift along the voltage axis similar to that observed for Na channels except that the magnitude of the shift was larger. A shift in this relationship was also observed for excised patches but the observable

* Present address: Max Planck Institut fur Biophysikalische Chemie, D-3400, Gottingen, Niklausberg, Am Fassberg – Postfach 968, F.R.G.

† Present address: Department of Physiology, Yale University School of Medicine, 333 Cedar Street, New Haven, CT 06510, U.S.A.

magnitude of the shift was smaller than that in the whole-cell recording mode. The asymptotic values of the charge *vs.* voltage relationship were similar for whole-cell and outside-out patches, as were the asymptotic values for the translocation time constants.

6. It is concluded that there are no fundamental differences in the properties of ionic channel and displacement currents between whole-cell membranes and excised membrane patches. The time-dependent shifts in the voltage dependencies of these properties are hypothesized to arise from both the slow dissipation of a Donnan-type potential between the cytoplasm and internal pipette solution and a change in the membrane's surface potential.

INTRODUCTION

The revolutionary electrophysiological techniques developed by Neher, Sakmann and their colleagues (Neher & Sakmann, 1976; Neher, Sakmann & Steinbach, 1978; Sigworth & Neher, 1980; Horn & Patlak, 1980; Hamill, Marty, Neher, Sakmann & Sigworth, 1981) for electrical recording from membranes of small cells and patches of cell membranes has opened the way for carrying out a large variety of experiments which were not previously possible. These techniques, referred to loosely as 'patch-electrode' techniques, enable one to record electrical signals from localized regions of membranes on cells, from the whole-cell membrane, and from 'inside-out' or 'outside-out' excised patches of cell membranes.

Because of the wide-ranging potential applications of the patch-electrode technique, it is important to determine that perturbations in the membrane which occur in the course of forming an excised patch do not significantly alter the membrane's electrical properties. For example, formation and excision of a membrane patch is likely to result in the same detachment from cytoskeletal elements and the same gross increases in membrane fluidity as have been observed for membrane 'blebs' (Tank, Wu & Webb, 1981, 1982; Wu, Tank & Webb, 1981). If the channels in the membrane are normally attached to the cytoskeletal elements (as the data of Almers, Stanfield & Stuhmer, 1983, suggest for Na channels in skeletal muscle fibres) or if the channel kinetics depend upon membrane fluidity (see Reyes & Latorre, 1979) then one might expect to observe different electrical properties for ionic channels in excised membrane patches than for those in whole-cell membranes. This concern has been substantiated by reports (Fenwick, Marty & Neher, 1982*b*; Cachelin, de Peyer, Kokubun & Reuter, 1983) that the voltage dependence of the inactivation kinetics and of the peak current of the Na channel are shifted along the voltage axis by up to -40 or -50 mV in excised patches as compared to whole-cell membranes.

In the present paper we report the results of a number of studies aimed at determining whether and how the electrical properties of excised membrane patches differ from those of the whole-cell membrane. For these studies we have used a clonal cell line (GH_3) from a rat anterior pituitary tumour (Tashjian, Yasumura, Levine, Sato & Parker, 1968) since these cells have been shown previously (Hagiwara & Ohmori, 1982) to be readily amenable to patch-electrode recording. In addition, these cells are readily maintained in culture and can be grown to contain large, consistent Na currents.

Preliminary reports of this work have been presented (Fox, Fernandez & Krasne, 1983; and Fernandez, Fox & Krasne, 1983*a*).

METHODS

Preparation. GH_3 cells, purchased from American Type Culture Collection (Rockville, MD, U.S.A.), were grown in culture flasks (250 ml). Synthetic culture medium Ham's F-10 was supplemented with 12·5 % horse serum and 2·5 % fetal calf serum (Irvine Scientific Products, Irvine, CA, U.S.A.) and innoculated with 2 % of a streptomycin–penicillin solution (GIBCO Laboratories, Grand Island, NY, U.S.A.; penicillin base = 10000 u./ml, streptocmycin base = 10000 μg/ml). The cultures were maintained at 37 °C in a humidified atmosphere of 5 % CO_2 and 95 % air. Cells in bottles were passaged to new flasks every 7–14 days, depending upon their rate of growth. Each time the cells were replated, only cells which had been firmly stuck to the side of the flask were transferred. This procedure was important in maintaining healthy cultures in which virtually 100 % of the cells tested showed large Na currents. Cells to be used for experiments were plated on glass cover-slips in Petri dishes. The medium in these Petri dishes was changed twice weekly, and cells could be maintained in this way for at least 1 month and still appear healthy. In order to readily form 'gigaseals' with patch electrodes, however, it was necessary to have changed the medium in the Petri dish within 3–4 days prior to use, and to leave at least 8 h after replacing the medium before starting the experiment. All experiments were performed at room temperature.

Electrodes. Patch electrodes were fabricated from low melting point, thin-walled glass capillaries ('micropipets'; van Waters & Rogers, Los Angeles, CA, U.S.A.). Pipettes were pulled on a vertical-type puller (David Kopf Instruments, Tujunga, CA, U.S.A., Model 700B) as described by Hamill *et al.* (1981). After pulling, the pipettes were coated with marine varnish to within 50–100 μm of the tip. The next day the pipette tips were fire polished to yield an opening of about 1–3 μm; the pipette resistances ranged between 1·5 and 3 Ω. The larger resistances were generally recorded when *N*-methylglucamine (*N*-MG) fluoride was used as the internal solution (see Table 1) as it has a lower conductivity than CsF, our other internal solution.

Recording and data processing. The terminology used in this paper is similar to that adopted by Fenwick, Marty & Neher (1982*a*). Three types of recording modes were employed: 'cell-attached', 'whole-cell' and 'excised outside-out patches'. In the cell-attached mode, a 'gigaseal' (pipette–membrane seal with resistance in the range of 10^9–10^{11} Ω; Hamill *et al.* 1981) is formed between the cell and the pipette; recording is across the small patch of membrane under the pipette tip. In the whole-cell mode, a gigaseal is formed with the cell as in cell-attached mode. The patch of membrane under the tip is ruptured using suction, providing access to the interior of the cell as well as allowing recordings of the electrical properties of the entire cell membrane. To obtain excised outside-out patches, the pipette is withdrawn from a cell which has previously been in the whole-cell mode. The seal resistance was usually significantly higher in the excised outside-out patch as compared to the cell-attached mode. In all cases, the resistances of the pipette–membrane seals were greater than 10 GΩ and typically were greater than 100 GΩ. Thus, the use of the term 'gigaseal' here implies a seal resistance $> 10^{10}$ Ω. The chamber volume was approximately 1 ml, but the solution level was kept lowered during recording to reduce the capacitance between the pipette and the bath.

The electronic circuitry of the patch-electrode amplifier was based on the block diagram found in Hamill *et al.* (1981). In our case, the feed-back resistor was 7·5 GΩ. For patch recordings the currents were either amplified with a variable gain amplifier (Model 113, Princeton Applied Research, Princeton, NJ, U.S.A.) or several traces were summed together. For all current recording in the time domain, the signal was passed through a six-pole Bessel low-pass filter (Frequency Devices, Haverhill, MA, U.S.A.) with an adjustable corner frequency, set to 2·5 kHz. Analog signals were digitized by a twelve-bit data acquisition module (DAS-250, Datel Systems Inc., Canton, MA, U.S.A.) and stored in a minicomputer (Nova 3/12, Data General, Southboro, MA, U.S.A.) which was also used for data analysis.

The command potentials fed to the patch clamp were generated by the computer.

For measurements involving whole-cell Na currents, P/4 or P/-4 procedures (Bezanillla & Armstrong, 1977) were used in order to subtract any linear capacitative and leakage currents from the current records with subtracting holding potentials typically more negative than −130 mV.

To subtract leak and capacitance from Na single-channel records small depolarizations, with no channel openings, were averaged (to improve the signal-to-noise ratio), scaled, and then subtracted from the single-channel records. Either 10 or 100 records were averaged. Records for leak and capacitance subtraction were acquired in blocks throughout the experiments to monitor changes in the leak and capacitance.

Displacement currents induced by 5×10^{-6} M of the lipophilic ion tetraphenyl borate (TPB) were measured with no leak or capacitance correction. The solutions used for these experiments totally suppressed all ionic currents. Each TPB current trace was sampled for a sufficiently long period to reach a definite steady state. Under these conditions any residual current found at the end of the current trace was assumed to be due to leak.

TABLE 1. Compositions of solutions (mM)

External			Internal		
	Ringer	Tris–Ringer		Cs solution	*N*-MG solution
NaCl	150	—	CsF	120	—
KCl	5	5	KF	—	—
$CaCl_2$	2	2	*N*-MG*	—	120
$MgCl_2$	1	1	$CaCl_2$	1	1
Glucose	10	10	$MgCl_2$	2	2
HEPES	10	—	HEPES	10	10
Trizma–7·6	—	150	EGTA	11	11
TTX (nM)	—	300			
Junction potentials (mV)	0	+7		−9	+2

N-MG refers to *N*-methylglucamine fluoride.

Solutions and measurement of liquid-junction potentials. The compositions of the internal (patch electrode) and external (bath) solutions used are listed in Table 1 along with the liquid-junction potentials measured relative to the Ringer solution. The liquid-junction potentials were measured by comparing the zero-current voltage in symmetrical Ringer solution and after replacing the bath solution with the solution to be tested. The reference electrode was always a 3 M-KCl–agar bridge. All data presented have been corrected for the liquid-junction potential.

Solutions were adjusted to pH 7·2. Then 10 mM-glucose was added and the solution filtered through a 0·2 μm Millipore filter. All experiments were done at room temperature. Aliquots of sodium tetraphenyl borate (Aldrich Chemical Co., Milwaukee, WI, U.S.A.) were added from a concentrated ethanolic solution; the ethanol concentration in the bath never exceeded 1 %. In the text, solutions are referred to according to the convention external solution//pipette solution.

Fluoride was always the main anion used to internally perfuse the GH_3 cells (the small amount of chloride being present solely to keep the Ag:AgCl wire reversible). With internal fluoride, whole cells were stable for hours. When we attempted to use chloride or aspartate as the internal anion the cells were typically only stable for a few minutes before the leak became too large to permit further experiments. This observation may be related to the fact that we used pipettes with large openings. An additional feature of cell behaviour in internal CsF (and to a lesser extent, *N*-MG) was that after rupturing the cell membrane the cell became leaky, but after several minutes of perfusion, the leak typically disappeared.

Scanning electron microscopy. Cells prepared for scanning electron microscopy were grown in plastic Petri dishes and fixed for 3 h in 2 % glutaraldehyde in 0·1 M-Na cacodylate buffer (470 mosmol/kg), at pH 7·2 and 20 °C. The cells were then treated with 2 % osmium tetroxide in 0·1 M-Na cacodylate buffer for 1·5 h and rinsed with buffer twice. The cells were dehydrated with a graded series of ethanol to 100 %. Small disks of the Petri dish containing cells were punched out and dried at the critical point of CO_2 in a Samdri pvt-3 critical point drying apparatus (Tousimis Research Corp., Rockville, MD, U.S.A.). Samples were mounted on stubs and coated with 100 Å gold–palladium with a Hummer I sputter coater (Technics, Alexandria, VA, U.S.A.). Samples were viewed with an ETEC Autoscan scanning electron microscope (ETEC Corp., Hayward, CA, U.S.A.) at 10 kV and micrographs were recorded on Polaroid type 55 negative films.

RESULTS

Cell-surface morphology

With a standard light microscope at 400 times magnification, individual GH_3 cells in culture appeared round, with outer diameters ranging from 10 to 20 μm. At this magnification the cell surfaces appeared rough, and the cell edges were not well defined. Using the increased resolution available in the scanning electron microscope (s.e.m.), a much more complicated surface morphology was revealed. Pl. 1 shows a s.e.m. micrograph of a GH_3 cell.

The GH_3 cell seen in Pl. 1 has features that are representative of the surface morphology typically observed under the s.e.m. for the cells used in the experiments reported in this paper. Even though there were variations among cells, the main features remain constant, namely that most cells were covered to varying degrees by microvilli (about 0·1 μm in diameter), blebs (0·1–2 μm in diameter), and ruffles (mild foldings of the cell-surface membrane). Projections extended from the cell surfaces to neighbouring cells as well as to the bottom of the Petri dishes.

Examination of Pl. 1 leads to a number of questions relevant to patch-clamp studies of GH_3 cells. The first is simply whether, given the variety of structures observed, formation of a gigaseal with a patch electrode is possible over the entire cell surface. The fact that we have had a high rate of success in forming such seals with cells such as those seen in Pl. 1 suggests that the ability to form gigaseals is not localized to any given surface structure(s), at least for these cells.

A second question is whether adequate voltage control of the whole-cell membrane can be achieved. For example, the access resistances associated with the cell-surface projections may be sufficiently large that the time for charging the membrane associated with these structures is much slower than that for the rest of the cell surface. Similarly, the current densities through the Na channels in these projections could be large enough for a significant fraction of the voltage drop to occur across the access resistances associated with these structures. The importance of these factors will be assessed by comparing the properties of Na currents in membrane patches and in whole-cell membranes later in this section.

Thirdly, it is evident that large underestimates of the total cell-surface area will occur if the cells are considered to be simple spheres (as they appear under the light microscope). Comparisons between GH_3 cells and other cell lines are difficult, in terms of current densities of capacitance per unit area, unless the actual membrane areas across which the currents are measured are known, as well as the passive linear electrical properties of the cells. For example, approximating the cells as simple spheres, Ozawa & Miyazaki (1979) have reported a value for the capacitance of GH_3 cells of approximately 9 $\mu F/cm^2$ based upon examination of the time constant for charging the cells to a given potential using an intracellular micro-electrode current clamp; on the other hand Matteson & Armstrong (1984) have reported values of 1–2 $\mu F/cm^2$ for these cells based upon analysis of the time constants in the whole-cell patch-clamp mode. Our own measurements of capacitance (Fernandez *et al.* 1983*a*) give values of 2–3 $\mu F/cm^2$ when the apparent radius of the cell, based upon light microscopy, is used.

Whole-cell Na currents

Fig. 1*A* shows a series of superimposed voltage-clamp records of the current responses of GH_3 cells to depolarizing test pulses. The holding potential was −84 mV and a P/4 procedure (Bezanilla & Armstrong, 1977) with a subtracting holding of −84 mV was used. These currents were completely abolished by 300 nM-tetrodotoxin

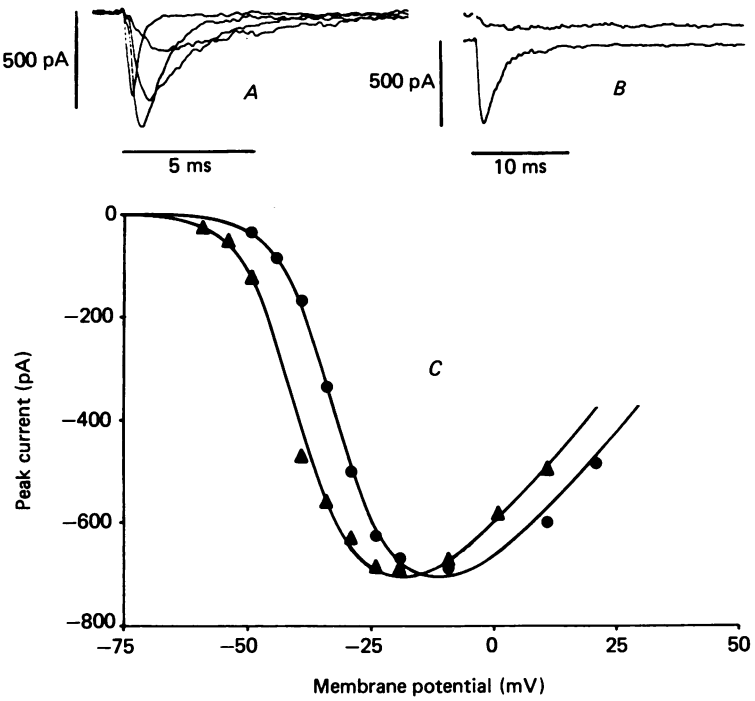

Fig. 1. Shifts along the voltage axis with time in the whole-cell Na currents. Solutions were Ringer//Cs. *A* shows superimposed traces of Na currents elicited by test pulses to −44 mV, −34 mV, −24 mV and +11 mV from a holding potential of −84 mV. A P/4 procedure was used with a subtracting holding of −84 mV. *B* displays two depolarizations in the same cell to −42 mV from a holding potential of −102 mV. The top trace was obtained immediately after going into the whole-cell recording mode while the bottom trace was taken 25 min later. We have displaced the two traces vertically, as indicated by the zero-current displacements, for the sake of clarity. The disparity in the traces can be accounted for by about 20 mV of difference in the voltage dependencies of the traces. *C* presents two peak Na current *vs.* test voltage (*I–V*) relationships obtained from data like that in *A*. ●, from data taken immediately after going into the whole-cell recording mode; ▲, from data obtained 20 min later.

(TTX) and were greatly diminished upon replacing 60% of the extracellular Na by Tris. The inward currents show the typical characteristics of inward Na currents found in other preparations. For large depolarizations inactivation is complete, no residual inward current being observed at long times. The voltage-clamp records one obtains for these cells were not, however, invariant with time. For example, Fig. 1*B* shows the Na currents observed for a depolarization to −42 mV within 2 min after

going into the whole-cell mode (upper trace) and 20 min later (lower trace). Clearly, the current had changed dramatically. This time dependence can be further analysed by examining the change in the peak inward current *vs.* voltage relationship (peak *I–V*) with time.

Using voltage-clamp data like that in the inset of Fig. 1*A*, a whole-cell peak *I–V* relationship was obtained. Fig. 1*C* shows two different peak *I–V* relationships obtained in the same cell. The filled circles represent the peak *I–V* measured after going into the whole-cell mode (referred to as 'time zero' but in fact occurring within 2–5 min after breaking the patch of membrane circumscribed by the electrode); the filled triangles represent a peak *I–V* obtained about 20 min later. The peak *I–V* curve has shifted about 10 mV in the hyperpolarizing direction in the 20 min between the data-gathering runs. Furthermore, individual records from the time-zero run are totally superimposable with those records from the 20 min data-gathering run obtained at about 10 mV more negative potentials. The shifting of the peak *I–V* along the voltage axis usually ceased within the first half-hour after going into the whole-cell mode. (Note, however, that the time course for this shift is much slower for patch electrodes with smaller tip diameters.)

Since our time-zero data-gathering run occurred about 2–5 min after going into the whole-cell mode, the cell's peak *I–V* had already been translocated somewhat along the voltage axis; indeed the peak *I–V* was shifting during the data-gathering run itself. This ambiguity about the initial peak *I–V* values makes it difficult to obtain estimates of the maximum shift possible. The maximum shifts in the peak *I–V* (as well as the Na channel kinetics; see below) we have observed were 20–25 mV.

Na current reconstructions from single-channel recordings

Single Na-channel currents are readily observable in outside-out patches excised from GH_3 cells, as shown in Figs. 2*A* and *B*. Fig. 2*A* shows three current traces elicited by voltage steps to −53 mV from a holding potential of −103 mV, while Fig. 2*B* shows three current traces for depolarizations to −43 mV from this same holding potential. Fig. 2*C* shows superimposed 'macroscopic' currents obtained by averaging 100 consecutive traces from one outside-out patch for each of four different potentials. Note that for the largest depolarization, inactivation is complete, with no residual inward current at the end of the pulse. By analysing reconstructions such as these, we have found activation of the current to be fastest for small and large depolarizations, with the slowest activation occurring at intermediate potentials; the relationship between activation and potential is thus bell-shaped. Clearly, these reconstructed currents behave in a very similar fashion to the whole-cell currents shown in Fig. 1*A*.

Fig. 3 directly compares current records from an outside-out patch (traces 1, 4 and 7), averaged currents reconstructed from the patch data (traces 2, 5 and 8), and whole-cell current traces (traces 3, 6 and 9) all in the same cell. Because the patch contained many channels, averaging only 50 or 100 records was sufficient to make the averages resemble the whole-cell currents. The whole-cell currents were measured approximately 20 min after going into the whole-cell mode and therefore most of the shift along the voltage axis had already occurred. At any given potential the current trace of the reconstruction is similar to that of the whole cell. Note, however, that

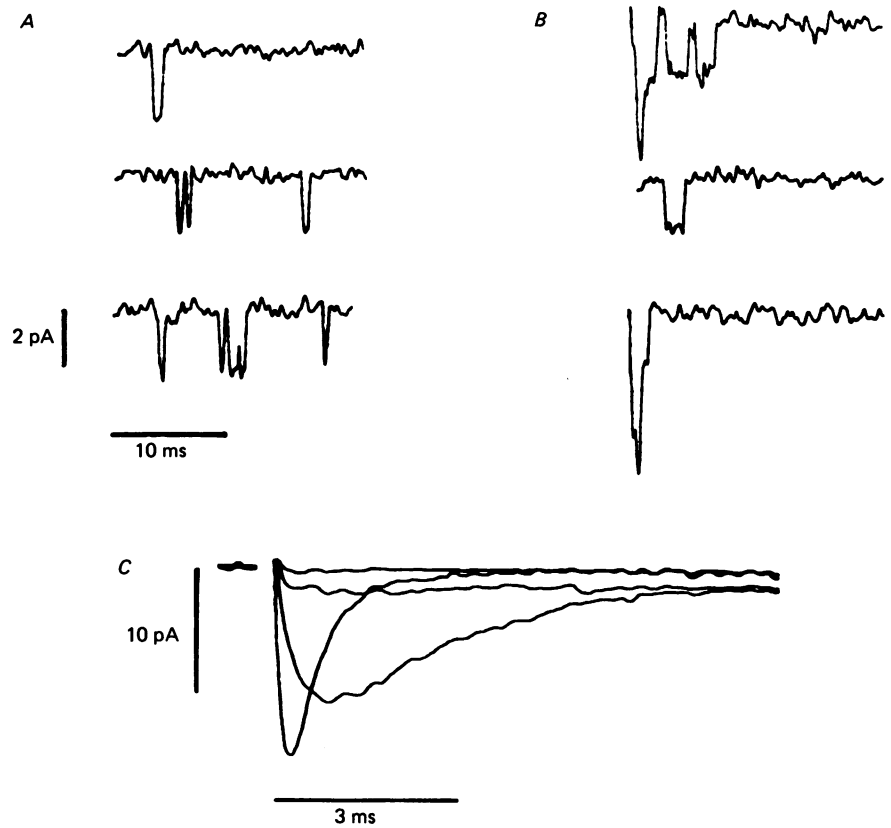

Fig. 2. Na currents in an excised outside-out patch. Solutions were Ringer//Cs. The traces in *A* and *B* show typical examples of single Na-channel current records elicited by a depolarization to −53 mV (*A*) or to −43 mV (*B*) from a holding potential of −103 mV. Leak and capacitance were subtracted from the records by averaging 100 traces of depolarizations to −73 mV, where only the linear properties of the membrane are observed, and then scaling and subtracting this result from the individual current records. Note that there is more than one channel in the patch and that for the records of *B*, the openings for the single Na channels are tending to cluster at the beginning of the traces. *C* shows Na currents reconstructed by averaging single channel traces of the type shown in *A* and *B*; 100 traces were averaged for voltage steps to −63, −53, −43 mV and 50 traces were averaged for a voltage step to −13 mV. Leak and capacitance were subtracted from each record before it was averaged as described for *A* and *B*. Note that the depolarizations to −53 and −13 mV yielded records with considerably faster times to the peak of the Na current than that to −43 mV, indicating that the activation time constant as a function of potential is bell-shaped. Also note that inactivation of the reconstructed current following a voltage step to −13 mV is complete.

the current traces from the whole cell are noisier than those of the reconstructions made by averaging data from the patch. This difference is due to the fact that a single sweep in the whole-cell mode has fewer activated Na channels than do 50 or 100 patch traces summed together. After multiplying by a scaling factor, the reconstructed patch records and the whole-cell records actually superimpose totally (indicating that the currents are kinetically identical) when the comparison is made using whole-cell

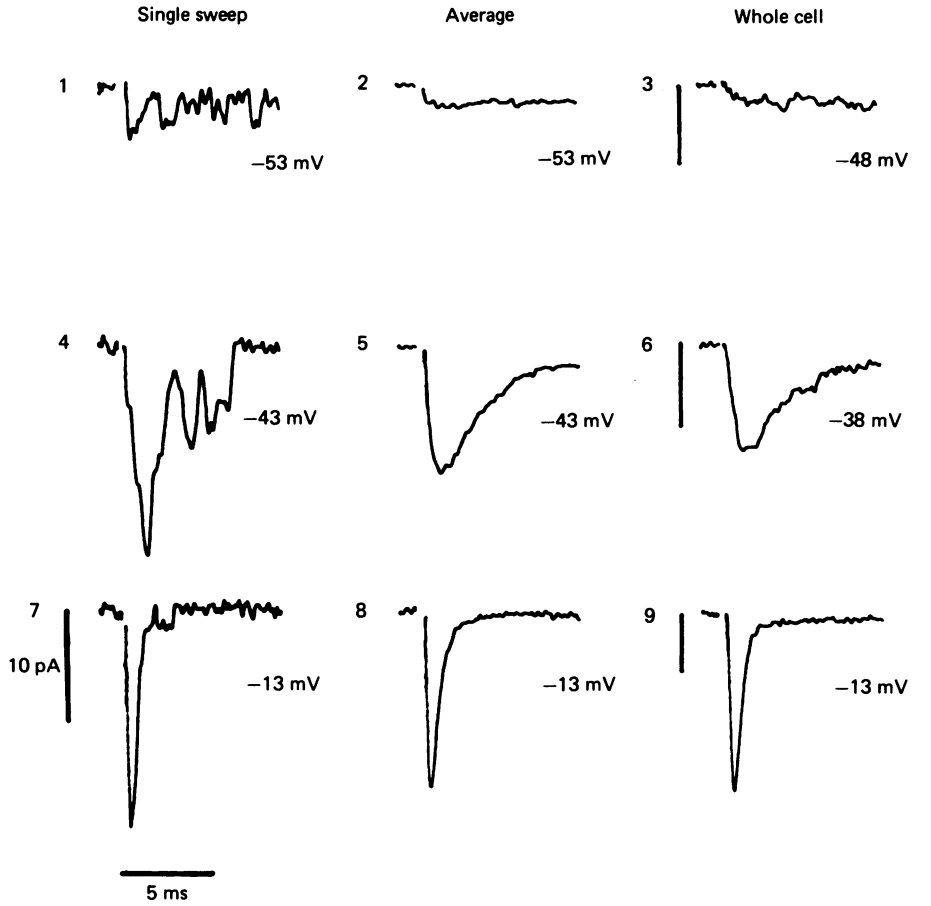

Fig. 3. Comparison of 'late' Na currents obtained from patch and whole-cell records in the same cell. The cell was kept in the whole-cell recording mode for 20 min before the whole-cell current data were gathered. A patch was subsequently excised and single-channel records were then taken. Solutions were Ringer//Cs. The holding potential was −103 mV. Traces 1, 4 and 7 show typical single-channel current records obtained from the excised patch in response to the depolarizing potentials indicated. Records 2, 5 and 8 show macroscopic current reconstructions obtained by averaging either 100 (the −53 mV and −43 mV traces) or 50 (the −13 mV trace) single-channel record traces from the same membrane patch. Capacitance and leak subtraction for the 'single sweep' and 'average' traces were as in Fig. 2. Traces 3, 6 and 9 show whole-cell currents elicited 20 min after whole-cell recording was begun by depolarizations to the potentials indicated. The vertical calibration marks for these traces equal 100 pA. The P/4 procedure was used with a subtracting holding of −103 mV. The patch from which the single-channel records of traces 1, 4 and 7 were taken had at least nine channels.

currents obtained at 5 mV more positive potentials than the averaged patch currents. This agreement indicates that the patch peak I–V was shifted 5 mV more negative than was that for the whole cell. When we have allowed a longer interval before taking the data in the whole-cell mode (so that the I–V shift was completed), we have observed no difference in potential between superimposable patch and whole-cell

records. The particular records in Fig. 3 were chosen for illustration, however, because they were significantly less noisy, and thus less ambiguous for the kinetic analysis presented below, than those from our experiments showing no shift.

Despite the excellent match between the whole-cell Na currents and the reconstruction data of the patch there is a problem intrinsic to this type of experiment. Namely, it takes quite a long time to record enough patch records for the averaging process

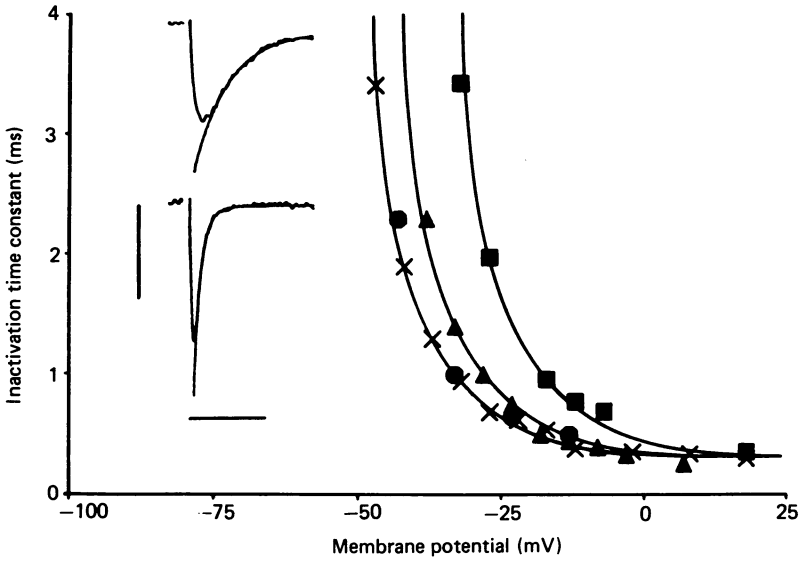

Fig. 4. Comparison of time constants of Na-current inactivation as a function of potential for both patch and whole-cell recordings. Two different whole cells and one patch are presented. Solutions were Ringer//Cs. ■, time constants from whole-cell data (fitted with a single exponential) collected immediately after going into the whole-cell recording mode; ●, the time constants for data collected from the same whole cell about 25 min later. ▲, for a different whole cell 20 min after going into the whole-cell recording mode. This cell then had a patch excised from it and single-channel data were obtained. The single channel data were averaged to reconstruct macroscopic Na currents from which time constants, of the current inactivation (fitted with a single exponential) represented by ×, were obtained. For ● and ■ the holding potential was −102 mV, while for ▲ and × the holding potential was −103 mV. P/4 was used on the data from which ▲, ● and ■ are taken, with a subtracting holding of −103 mV. Capacitance and leak were subtracted from the single-channel records as described in Fig. 2 in order to get the reconstructed Na currents used for ×. The inset shows examples of two of the reconstructed Na-current traces indicated by × and the fit of the Na-current inactivation by a single exponential. Calibration bars are 10 pA vertical and 5 ms horizontal.

to be effective. Therefore, there can be trends such as Na current rundown or other undetermined factors that can affect the data. Such trends result in significant variation in the scaling factor between the whole-cell Na currents and the reconstructed patch current from potential to potential. We tested for trends in the current elicited by a 90 mV depolarization by averaging the first ten records of data and then comparing this to the last ten records for the patch whose currents are illustrated in Fig. 3. At some point between taking the first ten records of the run and the last

ten, at least one other Na channel appeared. The loss or gain of a single channel in data used for averaging significantly changed the scaling factor, as a single channel produced a significant fraction of the total current of a patch. Thus *I–V* relationships based on data obtained from reconstructions of patch currents are difficult to obtain.

The inherent difficulties of using the amplitudes of the averaged patch data to compare with whole-cell data can be overcome if the kinetics of the inactivation process are compared instead. That the time constants of the inactivation process were well fitted by a single exponential can be seen in the inset of Fig. 4. Comparisons between whole-cell Na inactivation time constants as well as the inactivation time constants obtained from averaged patch records are shown in Fig. 4 as a function of potential. The squares show Na-current data taken from a whole cell within 2 min after breaking the patch, while the crosses correspond to whole-cell data taken from the same cell about 30 min later. The shift seen for these data is analogous to that seen for the peak *I–V*s in Fig. 1 and is about 15 mV. The triangles shown in Fig. 4 correspond to the time constants for the whole-cell currents illustrated in Fig. 3, which were obtained about 20 min after going into the whole-cell mode; the circles in Fig. 4 come from the reconstructed Na currents from the outside-out patch, shown in Fig. 3, excised from the same cell. (Note that data illustrated by squares and crosses are not from the same cell as those illustrated by triangles and circles.)

The agreement in Fig. 4 in the data from both the excised patch and the whole cell after completion of the shift is excellent. Indeed, we have found that for whole cells and/or patches from which we have recorded 30 min or more after going into the whole-cell mode, the time constants for the kinetics of inactivation have asymptoted to similar values at any given voltage.

TPB displacement currents in whole-cell and patch membranes

We have studied the displacement currents induced by TPB in GH_3 cell membranes. All ionic currents were eliminated by internally perfusing the cells with the *N*-MG solution and by using Tris–Ringer solution (which contains 300 nM-TTX) as the external solution. The cells were pre-incubated in Tris–Ringer solution containing 5 μM-TPB for at least 20 min prior to the beginning of recording in order to allow the TPB to equilibrate with the cell membrane.

After initiating whole-cell recording, TPB displacement currents were observed upon stepping the transmembrane voltage to different values from a holding potential of -91 mV; the amplitudes and time constants for decay of these currents were functions of the voltage step. Tail currents were obtained upon repolarizing cells to the holding potential after a depolarization for 100 ms. Typical whole-cell TPB tail currents are shown in the inset of Fig. 5. The amplitudes of the tail currents were proportional to the total charge which had been moved during the 'on' voltage step. When scaled, the tail currents superimposed for any given size of depolarization, indicating that the time constant for the 'off' current decay was always the same.

The P/-4 procedure (Bezanilla & Armstrong, 1977), for leak and capacitance subtraction, was not used in obtaining the TPB currents, as a subtracting holding potential more negative than -170 mV would have been needed in order to avoid any contributions to the capacitance from the TPB. With such a negative subtracting holding potential the cells always deteriorated rapidly. Even so, the TPB currents

were easy to separate out from the charging of the cell's geometric capacitance as the TPB currents were much slower. Thus, if the measurement of the tail amplitude was made about 1 ms (or more) after the beginning of the tail current, the artifact from the cell capacitance, which always had a time constant less than 100 μs, was negligible. For times longer than 1 ms the decay of the TPB currents was fit well by a single exponential.

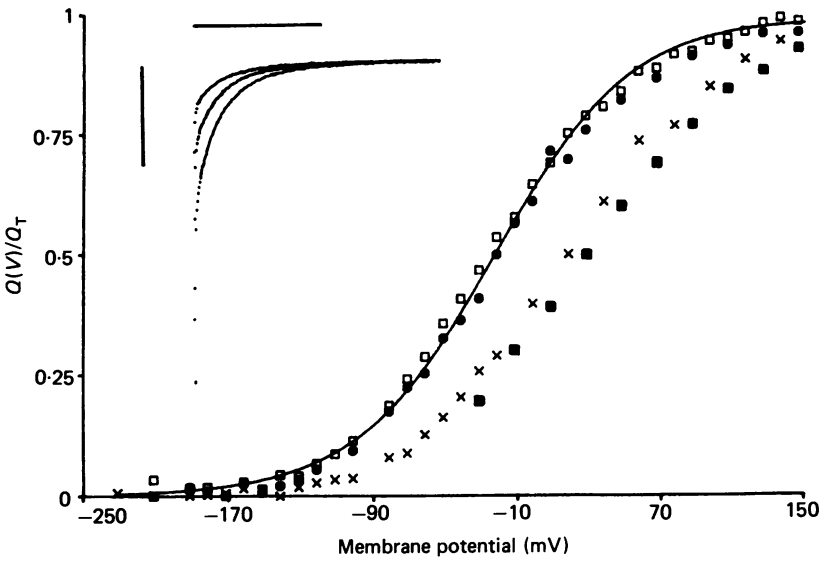

Fig. 5. Shifts with time of TPB-induced displacement currents in whole-cell membranes. Solutions were Tris–Ringer//*N*-MG with 5×10^{-6} M-TPB added to the bath. The inset shows tail currents obtained after the cell was repolarized to the holding potential of −91 mV following voltage steps to −61, −41 and −11 mV (top to bottom). Calibration bars are 200 pA vertical and 30 ms horizontal. Records of the type shown in the inset were fitted with a single exponential whose area was integrated to obtain the charge moved during the tail current. The charge moved was normalized and plotted as a function of the test depolarization (q–V). Points indicated by squares and crosses are from data taken immediately after going into the whole-cell recording mode. The first eight points of the data-gathering run are shown by ■ while the last twenty points are represented by ×. Each q–V took 5–7 min to complete. The q–V indicated by ● is from data acquired after 30 min, while the q–V indicated by □ is from data gathered 60 min after going into the whole-cell mode. The theoretical curve was drawn using eqn. (1) with $\alpha = 0{\cdot}63$ and the mid-point of the q–V, $V_h = -22$ mV. The asymptotic value for the total charge, Q_T, moved at large positive potentials is $5{\cdot}7 \times 10^{-12}$ C. Note that the theoretical curve fits both the 30 and 60 min data equally well. About 50 mV difference exists between the points for $Q(V)/Q_T = 0{\cdot}5$ for the time-zero run and the 30 and 60 min data-gathering runs.

The potential dependency of TPB charge movement (q) in the whole cell (TPB q–V), determined from tail currents as described above, is illustrated in Fig. 5. The crosses and filled squares correspond to measurements taken immediately after beginning whole-cell recording, the circles represent data taken 30 min later, while the open squares show the same measurements taken 60 min later, all on the same cell. The q–V shifted about 50 mV in the hyperpolarizing direction between time zero and time

30 min. This effect is similar, although larger in magnitude, to that observed for the Na currents shown in Fig. 1. There was no apparent shift between the 30 min and 60 min data runs, indicating that the cell had reached steady state during the first half-hour of whole-cell recording. It should be noted that the crosses and filled squares of the time-zero data do not form one continuous q–V but rather look like two distinct q–Vs. This is likely to be due to the shifting of the voltage dependence of the TPB tail currents during the data-gathering run (a run usually taking 5–7 min). The filled squares correspond to the first ten measurements taken during the run, while the crosses represent the subsequent measurements of the run. It is clear that there is a small shift between the crosses and filled squares.

The voltage dependency of TPB charge movement can be simply described by a system of TPB charges moving between two stable states with a first-order transition (see for example Reyes & Latorre, 1979). The total TPB charge moved at any given membrane potential, $Q(V)$, is given by

$$Q(V) = \frac{Q_T}{1+\exp\left(\frac{-e\alpha(V-V_h)}{kT}\right)}, \quad (1)$$

where Q_T is the total charge available to move, V_h is the membrane potential at which half of the total charge is in each stable state, α represents the fraction of the electric field through which the TPB charges translocate ($0 < \alpha \leqslant 1$), and e, k and T have their usual meanings. The continuous curve in Fig. 5 was generated using eqn. (1) with $V_h = -22$ mV and $\alpha = 0{\cdot}63$.

Relatively large displacement currents were also observed for TPB in excised, outside-out patches of membrane. The inset of Fig. 6 shows TPB tail currents recorded from an excised outside-out membrane patch using the same pulse procedure as described above for the whole-cell recordings. As for the whole cell, the time constant for the 'off' current decay is the same for all of the tail currents (at -91 mV) but the amplitude of the tail current is proportional to the total TPB charge moved during the prior 'on' voltage pulse. In order to ascertain whether the excised patches themselves could undergo shifts in their voltage dependencies, data for q–Vs were gathered immediately after patch formation (circles) and 30 min later (asterisks). Note that the voltage dependency of charge movement shifted by 19 mV towards more negative potentials during this period. The continuous curves in Fig. 6 were generated using eqn. (1) with $\alpha = 0{\cdot}65$ and $V_h = +11$ mV for the zero-time q–V (circles) and $V_h = -8$ mV for the q–V obtained after 30 min (asterisks). Notice that the parameter α is almost the same as that obtained for whole-cell measurements at 30 and 60 min, indicating that the slope of the q–V curve is the same in membrane patches and in whole-cell membranes.

As stated above, the displacement current generated by TPB upon stepping the membrane voltage to a given value from the holding potential has a time constant for decay which is a function of the voltage to which the membrane is stepped. Fig. 7 shows the voltage dependence of the time constants (fitted with a single exponential) in membranes from three different cells. The asterisks and triangles refer to measurements made on two different whole-cell membranes at least 30 min after the beginning of whole-cell recording so that the shift in the q–V relationship had

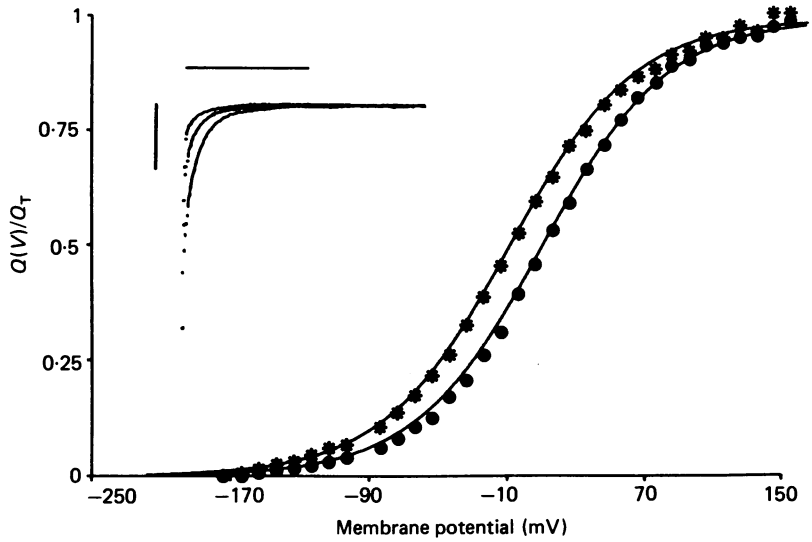

Fig. 6. Shifts with time of the TPB-induced displacement currents obtained from an excised, outside-out patch. Solutions were Tris–Ringer//*N*-MG with 5×10^{-6} M-TPB added to the bath. The inset shows typical tail currents obtained after repolarizing the cell to the holding potential of −93 mV following voltage steps to −63, −43 and −13 mV (top to bottom). The calibration bars are 50 pA (vertical) and 30 ms (horizontal). No capacitance or leak subtraction has been performed (see Methods). These tail currents were fitted by single exponentials which were integrated and normalized as described in Fig. 5. The patch used for this experiment was excised immediately after going into the whole-cell mode. The data points used for the q–V represented by ● were gathered as soon as the patch was excised (referred to as time zero). The q–V shown by * represents data taken 30 min later and shows the significant shift that excised patches can undergo. The theoretical curves were drawn with $\alpha = 0{\cdot}65$ for both the time-zero and 30 min data runs. The mid-point for the time-zero curve is at +11 mV while the mid-point for the 30 min data is at −8 mV. The asymptotic value for the total charge, Q_T, moved at large positive potentials is $1{\cdot}48 \times 10^{-12}$ C for each of the q–V curves. Each data trace shown in the inset is the sum of the current responses to three depolarizations.

already occurred; the circles correspond to measurements made on an outside-out patch from a third cell, after it too had completed the shift along the voltage axis.

Using the model from which eqn. (1) was derived, the time constant (τ), for charge translocation is given by (Fernandez *et al.* 1983*b*)

$$(\tau) = \frac{A}{\cosh\left(\frac{e\alpha(V - V_h)}{2kT}\right)}, \tag{2}$$

where α, V_h, e, k and T have the same meanings as in eqn. (1), and A is equal to the relaxation time constant evaluated at $V = V_h$ (the potential at which the time constants are the slowest, as well). The continuous curve in Fig. 7 has been drawn according to eqn. (2) with $\alpha = 0{\cdot}63$ and $V_h = -22$ mV. Note that these are the same values of the parameters as those used to fit the data in Fig. 5. The fact that the

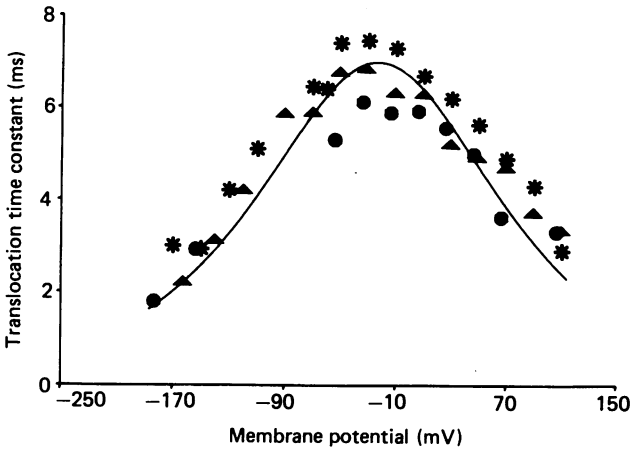

Fig. 7. Time constants of the TPB-induced displacement current decay as a function of potential recorded in the whole-cell and patch configurations. Solutions were Tris–Ringer//*N*-MG; 5×10^{-6} M-TPB was added to the bath. Data from two different whole cells (*, ▲) and an excised, outside-out patch (●) are shown. Single exponentials were fitted to the TPB current decay produced by test depolarizations to the potentials indicated on the abcissa from a holding potential of −89 (*), −90 (▲) or −93 (●) mV. All three sets of data were taken after the shifts of the q–V curves along the voltage axis were completed. Note that the variation between the patch and the whole-cells is comparable to that between the two different whole cells. The theoretical curve was drawn using eqn. (2) with $\alpha = 0{\cdot}63$, $\tau_{max} = 6{\cdot}8$ ms, and the mid-point of the curve $V_h = -22$ mV (these being the same parameters as were used to fit the data in Fig. 5).

patch data for both the slope of the q–V and the time constants of the currents are in agreement with the whole-cell data suggest that there are probably no fundamental differences in the lipid structure between outside-out patches and whole cells.

DISCUSSION

Systematic shifts in the voltage dependency of Na-channel gating and Na I–V relationships in excised patches as compared to whole-cell membranes have been noted previously (Fenwick *et al.* 1982*b*; Cachelin *et al.* 1983) and have been postulated by the former investigators to result from 'the changes in membrane structure that undoubtedly accompany the formation of cell-free patches'. In the present paper, we have systematically investigated the properties of Na currents in excised membrane patches and whole-cell membranes in order to determine whether the Na-channel properties seem different in these two forms of membrane. We have also compared displacement currents generated by TPB in these two forms of membrane in order to see whether the properties of the lipid matrix appear to be the same in excised membrane patches and whole-cell membranes (since the properties of Na channels themselves appear to be somewhat insensitive to variations in the properties of the membrane lipid matrix; see Fernandez, Bezanilla & Taylor, 1982). We have found that the voltage-dependent properties of both excised membrane patches and

whole-cell membranes appear to shift with time towards more negative potentials. This shift reaches an asymptotic value with time. The major conclusion which can be drawn from the results presented here is that, provided one waits for these shifts to occur, there is no apparent difference between ionic or displacement currents in excised outside-out membrane patches and whole-cell membranes. It seems likely, since such shifts are observed in both membrane patches and whole-cell membranes, that there would also be no differences in these currents if one could compare measurements made instantly after beginning whole-cell and patch recording; however, because of the finite amount of time required for measuring the voltage dependencies of these currents, data measured at short times are always contaminated by the shift. Indeed, depending upon the sequence of voltage steps applied, virtually any type of voltage dependency for Na-channel currents and time constants in membrane patches or whole-cell membranes might be observed when contaminated by this shift.

A major concern in evaluating the limits for which interpretations of whole-cell or patch membrane data are valid is the physical source of this shift. There are two major possibilities. The first is the shift is due to a time-dependent change in the potential difference between the patch pipette and the cytoplasm, as might originate from a junction potential or Donnan-type potential between them because of a slow exchange of ions. The second possibility is that the electric field within the membrane is changing over time due, for example, to desorption of anions or adsorption of cations bound to the inner membrane surface.

In the Appendix, we have examined the magnitudes of Donnan-type potentials which one might reasonably expect between the patch pipette and the cytoplasm. We have found that the shifts observed for the Na-channel data could be attributed to a Donnan-type potential if one assumes that virtually all of the ions in the pipette are mobile. The larger shifts observed for the TPB displacement currents require the assumption that most of the cations in the patch pipette are 'immobile' (requiring 30 min or more to diffuse into the cell). A major difference existed in the internal solution of the patch pipette between these two experiments in that the CsF solution of Table 1 was always used in measuring Na currents whereas the *N*-MG solution was used in measuring TPB displacement currents. If *N*-MG were virtually 'immobile' in either the pipette or cytoplasm solution, so that it took approximately 30 min to equilibrate with the cytoplasm, then we could conclude that the differences which we observe for the two types of experiments are due to differences in Donnan-type potentials. However, at the present time it seems unreasonable to suppose that the mobility of *N*-MG could be so restricted in either the pipette solution or the cytoplasm. Thus, whereas some component of the shifts in the voltage dependencies of Na and TPB currents is likely to arise from a Donnan type of potential, the magnitude of the shifts, especially for *N*-MG internal solutions, larger than those calculated in the Appendix, argues that these shifts also represent adsorption or desorption of ions bound to the inner membrane.

From our measurements, there appears to be a different magnitude of shift over time for the voltage-dependent properties of Na channels as compared to those for TPB currents. One possible source of this discrepancy might arise from a necessary delay (approximately 5 min) in initiating measurements of Na currents (but not TPB

currents) immediately after establishing continuity between the patch pipette and the cell interior. This delay was caused primarily by the fact that GH_3 cells tended to become very leaky for a few minutes after rupturing the patch membrane in Cs but not in *N*-MG solutions (see Methods).

One factor which might be related to a difference in shifts is differential interactions of Cs and *N*-MG with the membrane. Selectivity in the effects of external anions in altering the surface charge near Na channels have been reported previously (Dani, Sanchez & Hille, 1983), and a similar phenomenon may contribute to the shifts we observe here. Alternatively, a difference in the magnitude of the shifts seen for the TPB q–V relationship and the Na channel I–V or q–V relationships could involve differential desorption (or adsorption) of an hydrophobic ion near Na channels as compared to other regions of the membrane. For example, the electric field measured using extrinsic charge carriers in axon membranes (Hall & Cahalan, 1981; Benz & Conti, 1981; Benz & Nonner, 1981; Fernandez *et al.* 1983*b*) is quite different from that measured using Na-channel currents (Hille, 1968; Gilbert & Ehrenstein, 1969; Chandler, Hodgkin & Meves, 1965).

Comparisons can also be made between the Na-channel and TPB data presented here and analogous data from other systems. For example, the values for α and V_h in eqns. (1) and (2) when measured in the whole cell or the membrane patch after the shift are remarkably similar to those measured ($\alpha = 0{\cdot}63$ and $V_h = -15$ to -20 mV) for dipicrylamine in perfused squid axon membranes (Fernandez *et al.* 1983*b*) but are very different from those reported ($\alpha = 0{\cdot}8$ and $V_h = 0$) for symmetrical planar lipid bilayer membranes (Andersen & Fuchs, 1975). The parameter α is related to the position of the adsorption plane for TPB in the membrane's electric field and may well depend upon factors such as the presence of intrinsic membrane proteins. V_h is an indicator of the difference in electrical and/or standard chemical potentials between the adsorption planes for TPB on either side of the membrane in the absence of an applied potential. Such a difference could arise, for example, because of a difference in the electrostatic potentials at the outer and inner membrane surfaces or because of a difference in lipid or protein compositions at the two membrane surfaces; however, one could artifactually infer such a difference to be present if there were a junction potential between the voltage-measuring electrode and the cytoplasm (in which case a voltage difference would actually occur at this junction and not across the membrane). Interestingly, in frog node of Ranvier, in which dialysis of the intracellular compartment is incomplete due to time limitations, the values of V_h measured by extrinsic probes appear to be closer to those which we find at time zero, before any significant shift has taken place; thus, the value of V_h for TPB in frog node of Ranvier is more positive than 0 mV (Benz & Nonner, 1981) and the value of V_h for a methyl ester derivative of alamethicin (which shows symmetrical I–V curves for positive and negative potentials across symmetrical planar lipid bilayers) is +25 mV in the same preparation (Hall & Cahalan, 1981). The maximum of the Na-channel I–V curve for chromaffin cells, based upon whole-cell recording, is between 0 and +10 mV (Fenwick *et al.* 1982*b*), although recently shifts of about 10–20 mV to more negative potentials have been observed over a 30 min period (Marty & Neher, 1983).

Pharmacological isolation and maintenance of ionic channels

In the course of this study, we found that the use of internal fluoride in the patch pipette dramatically increased the time over which recordings could be made from these cells from typically less than 10 min (with chloride or aspartate in the pipette) to more than 2 h. This effect is similar to that observed in the squid giant axon for which internal fluoride is necessary for the maintenance of ionic currents without significant deterioration of the cell membrane over time. In addition, when other internal anions (chloride and aspartate) have been used, Na currents have been observed (by ourselves as well as by Hagiwara & Ohmori, 1982) to be highly variable in magnitude from cell to cell and are observed with decreasing frequency the longer the cells have been in culture. When fluoride was used in the patch pipette, all GH_3 cells showed clear Na currents in the whole-cell recording mode. (We have used as low as 50 mM-fluoride in the patch pipette and found the same results.) These observations, which have also been made on other cells (see, for example, Kostyuk, Krishtal & Pidoplichko, 1975) suggest a possible interaction between internal anions and Na channels (or perhaps between proteolytic enzymes and anions) such that certain anions can stabilize Na channels.

Good pharmacological isolation of inward Na currents has been achieved by using CsF as the major salt in the patch pipette with Cs blocking K currents and fluoride removing Ca currents. Evidence for this was the absence of any time-dependent ionic currents either following inactivation of the Na currents at large depolarizations or when the bath contained 300 nM-TTX. For experiments on TPB currents, internal *N*-MG was used instead of Cs and was just as effective in removing delayed-rectifier K currents, even for records obtained at the shortest times possible after establishing continuity between the patch pipette and the cell interior (about 30 s). Since *N*-MG is apparently impermeant in delayed-rectifier K channels but does not block them (M. White & F. Bezanilla, personal communication), this observation suggests that for these ions and the large-tip-diameter pipette we used, exchange with the cytoplasm was rapid.

When the patch pipette did not contain *N*-MG it was usual to observe the appearance of a large variety of sizes of ionic current fluctuations, over the whole voltage range examined, typically within 10–15 min after formation of an outside-out patch. These current fluctuations, which appear to reverse at 0 mV, rapidly become a problem when attempting to record from single, ion-specific channels. We believe that the appearance of these channels reflects the deterioration of the membrane patch and is equivalent to what is commonly called 'leakage' in macroscopic measurements. This speculation is supported by the fact that they are not present immediately after formation of the patch and that they do not appear at all when *N*-MG, rather than Cs or K, is used as the internal cation. In squid giant axon as well, perfusion with *N*-MG greatly reduces the 'leakage' current observed over a prolonged period of time.

APPENDIX

As stated in the Discussion, there appears to be a rapid exchange between the major ions in the pipette and at least the small ions in the cytoplasm. However, there may be a significant concentration of large, relatively immobile anions in the cytoplasm, such as those which give rise to Donnan potentials, which require much longer times (e.g. 30 min) to exchange. If so, at short times after initiating whole-cell recording, a pseudo-equilibrium will exist between the cytoplasm and the internal solution in the pipette, and these slow-moving anions will give rise to a potential which can be calculated in the same manner as a Donnan potential. One can estimate the magnitude for this Donnan-like potential from the concentrations of permeant ions inside the patch pipette and estimates of the concentrations of large, impermeant anions in the cytoplasm of other cells.

As an example, we shall use the estimate of intracellular impermeant ion concentrations of 163 mM for mammalian skeletal muscle (MacKnight & Leaf, 1978). Because the internal volume of the patch pipette is many orders of magnitude larger than that of the cell, we can assume that the concentrations of ions in the pipette remain unchanged. The mobile ions will rearrange themselves between the internal pipette solution and the cytoplasm to satisfy the conditions for the Donnan equilibrium. These conditions are that electroneutrality exist in the cytoplasm and in the pipette and that the ratio of concentrations of permeant cations of a given valence in the pipette to those in the cytoplasm be the reciprocal of the ratio of permeant anions of the same valency. For simplicity, we have assumed that 2 mM-Mg is equivalent to 4 mequiv monovalent cations that EGTA and its Ca complex do not contribute to charge redistribution. Also, at the pH of these experiments, approximately half of the HEPES is in the charged form. Thus, for the patch pipette, the total concentrations of permeant cations, C_e, and anions, A_e, are approximately

$$C_e = 131 \text{ mequiv}, \tag{A1}$$

$$A_e = 131 \text{ mequiv}. \tag{A2}$$

The Donnan equilibrium assumptions stated above can be written as

$$C_i = A_i + 163 \text{ mequiv}, \tag{A3}$$

and

$$C_e \cdot A_e = C_i \cdot A_i, \tag{A4}$$

where C_i and A_i refer to the concentrations of internal, mobile cations and anions, respectively. Substituting eqns. (A1)–(A3) into (A4) yields the values $C_i = 236$ mequiv and $A_i = 73$ mequiv. For this distribution of mobile cations and anions, the calculated Donnan potential is -15 mV (cytoplasm relative to pipette solution). This value is significantly less than the shift we observe for the TPB q–V, although it is similar to the values which we have observed for the Na I–V relationship.

The difference between the calculated Donnan potentials and the changes in potential during the shifts in the Na I–V and TPB q–V relationships are unlikely to be due to an underestimate of the concentration of immobile anions inside the cell

since large increases in this value make only small changes in the calculated potential (e.g. for the same ion concentrations in the pipette, 200 mequiv of immobile anions inside the cell would yield a Donnan potential of −18 mV). However, a large increase in the expected potential results if the concentration of mobile cations in the electrode is reduced. Thus, if *N*-MG were an immobile cation, C_e in eqn. (A1) would approximately equal 9 mequiv and the resultant, calculated Donnan potential (for 163 mequiv immobile anions inside the cell) would be −74·6 mV which is even larger than the largest shift observed for the TPB q–V. (Of course, such a calculation is only a very crude estimate in this case since much of the mobile cation concentration in the pipette solution is due to Mg which has been treated as the same number of equivalents of monovalent cations.) Because outward K currents are not observed when the patch pipette contains *N*-MG solution, we presume that *N*-MG exchanges rapidly with the ions in the cytoplasm; however, it is possible that *N*-MG is immobile and that other ions, such as Mg, displace the K in the intracellular solution, resulting in a larger Donnan potential.

It is a pleasure to thank Drs Sergio Ciani, Susumu Hagiwara and Richard Horn for many helpful discussions and suggestions throughout the course of this work. This research was supported by American Heart Association Fellowships to J.M.F. and A.P.F. and by grants from the National Institutes of Health (HL20254) and the Muscular Dystrophy Association to S.K.

REFERENCES

ALMERS, W., STANFIELD, P. R. & STUHMER, W. (1983). Lateral distribution of sodium and potassium channels in frog skeletal muscle: measurements with a patch-clamp technique. *Journal of Physiology* **336**, 261–284.

ANDERSEN, O. S. & FUCHS, M. (1975). Potential energy barriers to ion transport within lipid bilayers. Studies with tetraphenylborate. *Biophysical Journal* **15**, 795–830.

BENZ, R. & CONTI, F. (1981). Structure of the squid axon membrane as derivated from charge-pulse relaxation studies in the presence of adsorbed lipophilic ions. *Journal of Membrane Biology* **59**, 91–104.

BENZ, R. & NONNER, W. (1981). Structure of the axolemma of frog myelinated nerve: relaxation experiments with a lipophilic probe ion. *Journal of Membrane Biology* **59**, 127–134.

BEZANILLA, F. & ARMSTRONG, C. (1977). Inactivation of the sodium channel. I. Sodium current experiments. *Journal of General Physiology* **70**, 549–566.

CACHELIN, A. B., DE PEYER, J. E., KOKUBUN, S. & REUTER, H. (1983). Sodium channels in cultured cardiac cells. *Journal of Physiology* **340**, 389–401.

CHANDLER, K., HODGKIN, A. & MEVES, H. (1965). The effect of changing the internal solution on sodium inactivation and related phenomena in giant axons. *Journal of Physiology* **180**, 821–836.

DANI, J., SANCHEZ, J. & HILLE, B. (1983). Lyotropic anions. Na channel gating and Ca electrode response. *Journal of General Physiology* **81**, 255–281.

FENWICK, E. M., MARTY, A. & NEHER, E. (1982*a*). A patch-clamp study of bovine chromaffin cells and of their sensitivity to acetylcholine. *Journal of Physiology* **331**, 577–597.

FENWICK, E. M., MARTY, A. & NEHER, E. (1982*b*). Sodium and calcium channels in bovine chromaffin cells. *Journal of Physiology* **331**, 599–635.

FERNANDEZ, J. M., BEZANILLA, F. & TAYLOR, R. E. (1982). Effect of chloroform on charge movement in the nerve membrane. *Nature* **297**, 150–152.

FERNANDEZ, J. M., FOX, A. & KRASNE, S. (1983*a*). Cell surface morphology and the patch clamp technique. *Neuroscience Abstracts* **9**, 1188.

FERNANDEZ, J. M., TAYLOR, R. E. & BEZANILLA, F. (1983*b*). Induced capacitance in the squid giant axon. *Journal of General Physiology* **82**, 331–346.

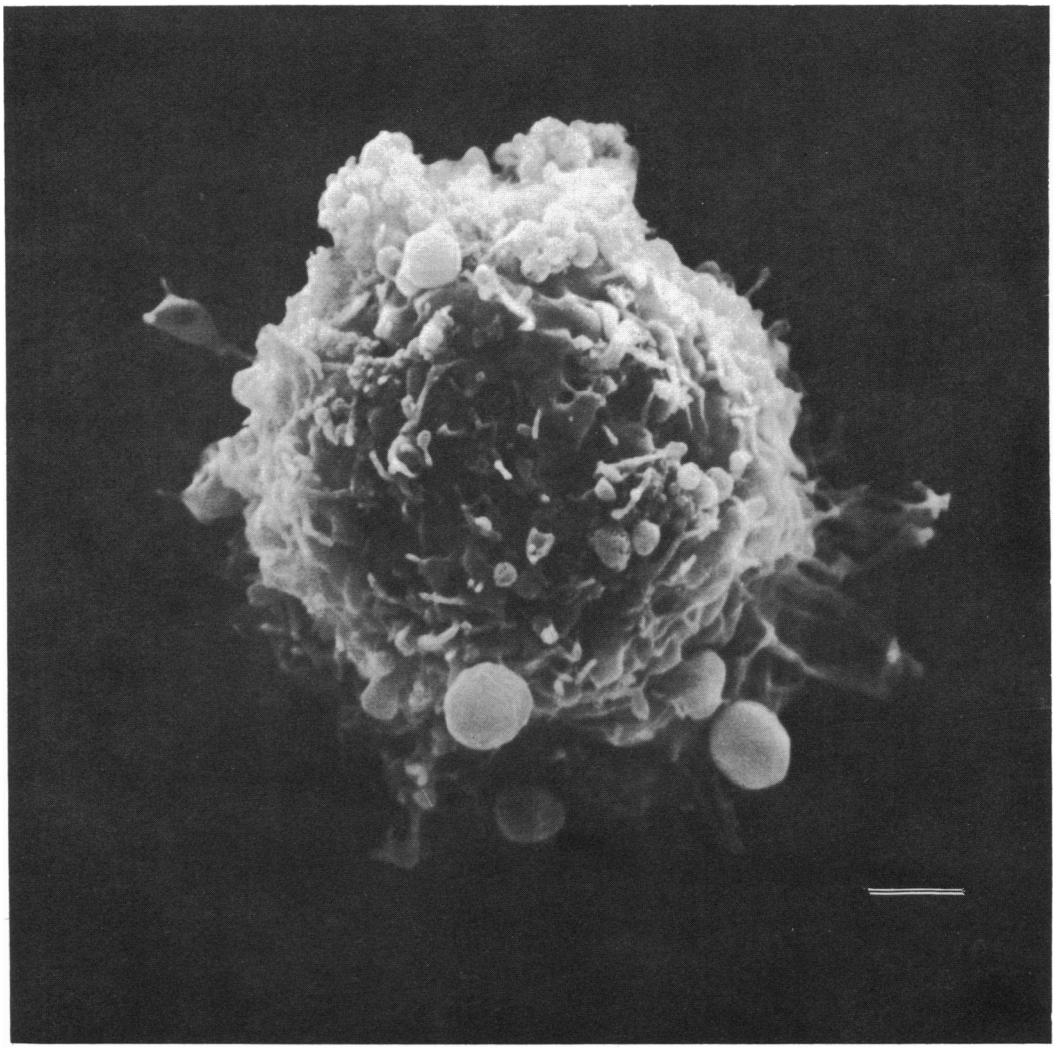

FOX, A., FERNANDEZ, J. M. & KRASNE, S. (1983). Membrane patches and cell membranes: a comparison. *Neuroscience Abstracts* **9**, 1188.

HAGIWARA, S. & OHMORI, H. (1982). Studies of calcium channels in rat clonal pituitary cells with patch electrode voltage clamp. *Journal of Physiology* **331**, 231–252.

HALL, J. & CAHALAN, M. (1981). Alamethicin reveals internal surface charges at frog Node of Ranvier. *Biophysical Journal* **33**, 62a.

HAMILL, O. P., MARTY, A., NEHER, E., SAKMANN, B. & SIGWORTH, F. J. (1981). Improved patch-clamp techniques for high-resolution current recording from cells and cell-free membrane patches. *Pflügers Archiv* **391**, 85–100.

HILLE, B. (1968). Charges and potentials at the nerve surface. Divalent ions and pH. *Journal of General Physiology* **51**, 221–236.

HORN, R. & PATLAK, J. (1980). Single channel currents from excised patches of muscle membrane. *Proceedings of the National Academy of Sciences of the U.S.A.* **77**, 6930–6934.

KOSTYUK, P. G., KRISHTAL, O. A. & PIDOPLICHKO, V. I. (1975). Effect of internal fluoride and phosphate on membrane currents during intracellular dialysis of nerve cells. *Nature* **257**, 691–693.

MACKNIGHT & LEAF, A. (1978). Regulation of cellular volume. In *Physiology of Membrane Disorders*, ed. ANDREOLI, T. E., HOFFMAN, J. F. & FANESTIL, D. D., pp. 315–334. New York: Plenum Press.

MARTY, A. & NEHER, E. (1983). Tight-seal whole cell recording. In *Single-Channel Recording*, ed. SAKMANN, B. & NEHER, E., pp. 107–121. New York: Plenum Press.

MATTESON, D. R. & ARMSTRONG, C. (1984). Na and Ca channels in a transformed line of anterior pituitary cells. *Journal of General Physiology* **83**, 371–394.

NEHER, E. & SAKMANN, B. (1976). Single-channel currents recorded from membrane of denervated frog muscle fibres. *Nature* **260**, 799–801.

NEHER, E., SAKMANN, B. & STEINBACH, J. H. (1978). The extracellular patch clamp: a method for resolving currents through individual open channels in biological membranes. *Pflügers Archiv* **375**, 219–228.

OZAWA, S. & MIYAZAKI, S. (1979). Electrical excitability in the rat clonal pituitary cell and its relation to hormone secretion. *Japanese Journal of Physiology* **29**, 411–426.

REYES, J. & LATORRE, R. (1979). Effect of the anaesthetics benzyl alcohol and chloroform on bilayers made from monolayers. *Biophysical Journal* **28**, 259–280.

SIGWORTH, F. J. & NEHER, E. (1980). Single Na^+ channel currents observed in cultured rat muscle cells. *Nature* **287**, 447–449.

TANK, D. W., WU, E. S. & WEBB, W. W. (1981). Enhanced mobility of acetylcholine receptor and membrane probes in muscle membrane blebs. *Biophysical Journal* **33**, 74a.

TANK, D. W., WU, E. S. & WEBB, W. W. (1982). Enhanced molecular diffusibility in muscle membrane blebs: Release of lateral constraints. *Journal of Cell Biology* **92**, 207–212.

TASHJIAN JR, A. H., YASUMURA, Y., LEVINE, L., SATO, G. H. & PARKER, M. L. (1968). Establishment of clonal strains of rat pituitary tumor cells that secrete growth hormone. *Endocrinology* **82**, 342–352.

WU, E. S., TANK, D. & WEBB, W. W. (1981). Lateral diffusion of concanavalin A receptors and lipid analog in normal and bulbous lymphocytes. *Biophysical Journal* **33**, 74a.

EXPLANATION OF PLATE

Scanning electron micrograph of a GH_3 cell. This cell is representative of those used in the patch pipette experiments. Cells were treated as described in the text. The bar equals 2 μm.